HYDRODYNAMICS FLOW VISUALIZATION IN OIL TRAP FILTERS

Herbert Carlos Gonçalves – herbert@dem.feis.unesp.br
Edson Del Rio Vieira – delrio@dem.feis.unesp.br
Universidade Estadual Paulista – Unesp – Departamento de Engenharia Mecânica
Cx. P. 31, – 15385-000 – Ilha Solteira, SP, Brasil

Abstract. *Airflow with oil fog occurs in many exhaust systems of kitchens, restaurants and food processing industries and others related industrial facilities. Separation of the oil from the air requires the use of expensive filter systems and in high oil concentration cases, the use of pre-filters are indispensable. Oil trap filters (also named inertial filter) are intensively utilized like a pre-filter, in those cases, since they are cheap and provoke low-pressure loss. An experimental visualization study in hydrodynamic medium of the flow around a semi-tube array simulating a oil trap filter has been carried out in this work as a first effort in order to understand the operating principle of an inertial filter. Experiments have been carried out in a vertical low turbulence hydrodynamic tunnel operated in blow-down mode. Still images have been captured in 35 mm chemical film using the liquid dye injection flow visualization technique.*

Keywords: *Flow visualization, Vortex shedding, Image processing, Oil trap filter*

1. INTRODUCTION

Airflow with oil fog occurs in many exhaust systems of industrial kitchen, or in big restaurants. Generally, the oil fogs result of the cooking in hot oil process. Oil fog is also formed in industrial facilities of machining process. In this case, soluble cooling oil, utilized to facilitate the cutting of metals, is continually sprayed forming oil micro drops carried by environment air streams.

The presence of food oil in the air is very dangerous due to the oil incrust in exhaust-duct walls that allows for development and proliferation of insects and many micro organisms prejudicial to human health and incompatible with a kitchen environment. Additionally, problems with fire are fairly common in food oil and air exhaust systems and oil incrusts also difficult the action of mechanic actuators in automatic doors to prevent damage fire propagation. Because of those problems, and to minimize the atmospheric air pollution, exhaust system of big kitchens requires filters installation.

Machining process exhaust systems also need filters since the expensive cooling soluble oil, utilized to help in cutting metals, can be reused several times, after properly processed.

On the other hand, a crescent preoccupation with environment issues forces towards an exhaust of clear and purified air. No rare, kitchen exhaust provokes, in high-density

population centers, relationship problems with neighborhood due to the characteristic odor emanations.

In these two cases, where a high oil micro-drop concentration is present, commonly water aspersion in form of a curtain or cyclone type filters employment is needed. But, unfortunately, both those systems require expensive costs in installations, maintenance and energy consumption. Additionally, water curtain and cyclone type filters introduce a high-pressure loss, provoking the installation of large apparatus and high power motors. The use of conventional paper air filters in the exhaust ducts is compromised by frequent saturation of the filter element due to the high oil concentration. In this case, the use of oil trap filters, as a preliminary filter, is absolutely necessary.

Filters of oil trap type (also known by technical people as inertial filters) operate according to the principle showed in Figure 1. In this apparatus, an air and oil-drop stream, into the exhaust duct, is conducted along an array of cylinders with a half-cane cross section. The oil - air flow tends to contour the gutter array, but the oil drops fail to contour perfectly the filter geometry, so that they collide against the walls or are arrested in the recirculation wake downstream the filter and finish shocking against the leeward wall of the cylinder array. The oil drops that are captured along the cylinder walls are conducted to a recipient by gravitational action at an angle (α) formed by the bottom duct wall and the filter depicted in Figure 1.

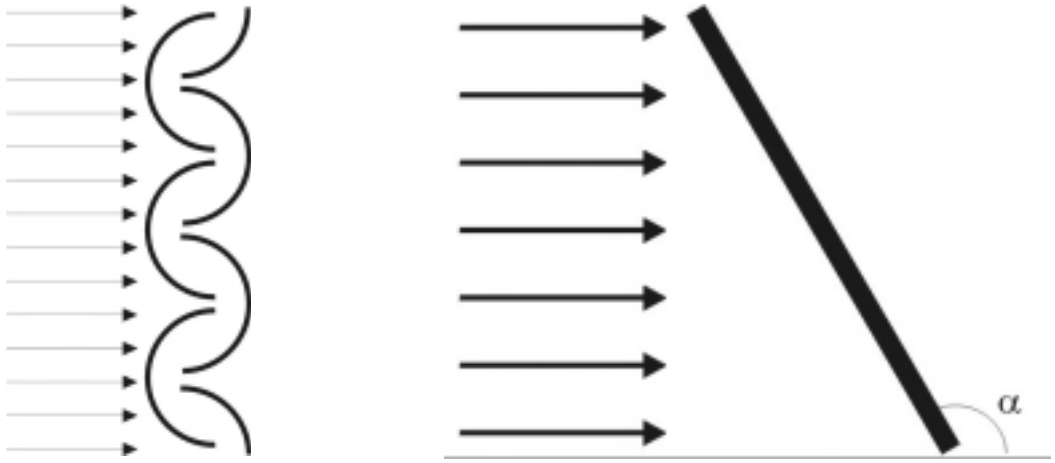

Figure 1 – Inertial filter – the oil-air flow is deflected by semi-tubes array capturing the oil drops.

A preliminary study utilizing a flow visualization tool in hydrodynamic medium in order to gather the first qualitative information about operating principle of oil trap filters and identify the oil trap mechanisms are the principal goals of this work.

2. DROPLETS DEPOSITION MECHANISMS

Cooking in hot oil produces smokes of characteristics odor. The word “smoke” is frequently employed in a broad sense, and includes a variety of smokelike materials such as vapor, fumes, and mists. Smoke is also referred in the sense of aerosol, which is defined as either a fine liquid or fine solid suspension in gas. A great deal of interest has been focused on the properties and generation of aerosols due to their close relationship to meteorology, air pollution, clouds, smokes, fuel combustion, etc. Aerosol oil drops have particle diameter on the order of the wavelength of the incident light, from approximately 0.03 to 1.0 μm.

Although many substances have particles sizes below 1.0 μm, the most usual ones are the tobacco smoke (0.01 - 1.0 μm) and rosin smoke (0.01 - 1.0 μm). The oil droplets have a long residence time in the atmosphere because of their small diameters.

According to Schatzmann (1999), gravitational, electrostatic and flow-induced forces influence the deposition of small drops in surfaces. Since electrostatic forces are of minor importance, it remains sedimentation, direct impact and diffusion like flow-induced forces to be accounted for. Sedimentation happens when drop movement is mostly driven by its weight and therefore it is significant only to big drops. Droplet impact is a consequence of inertial action, the droplets failing to follow precisely the streamlines and consequently impacting against a solid obstacle. Diffusion occurs when very small drops escape from direct impacting at the front of the target, but may be trapped in the obstacle wake and thrown against the leeward obstacle side by turbulent and molecular diffusion.

3. FLOW VISUALIZATION TOOLS

Flow visualization is perhaps the most useful experimental tool in obtaining, by a fast and cheap way, qualitative information on flow structure. Many experimental flow visualization techniques are described in the technical literature, only to exemplify, Yang (1989), Merzkirch (1987), Goldstein (1976) and Freymuth (1993), among several other references.

In a broad sense, flow visualization is more easily performed in aqueous than in air medium, since there are many ways of making water visible, by means of different color inks, gaseous bubbles or solid dust in suspension. Werlé (1973) details several hydrodynamics facilities and flow visualization techniques applicable in water.

Generally, water tunnels have smaller test section dimensions when compared with aerodynamic tunnels. Therefore, in the water tunnel case, small bodies tested with moderate blockage ratios, implies relative low Reynolds numbers. In spite of the water kinematics viscosity might be less than 15 times the air kinematics viscosity in the same temperature, the Reynolds numbers obtained in hydrodynamics tunnels are smaller than the Reynolds obtained in aerodynamics tunnels. Relatively lower Reynolds numbers stands a serious restriction to the use of water tunnels in substitution to aerodynamic tunnels. Erickson (1980), motivated by the possibility of vortex flow visualization in hydrodynamics medium, debates, in details, this problem of low Reynolds tests in water tunnels and the care in the results interpretation.

In this paper, in order to obtain the preliminary results of the effort work for knowledge of operational mechanism of inertial filters, two flow visualization techniques utilizing an opaque liquid dye were employed. In the first method, the traditional direct injection technique has been used. In this technique a long hypodermic needle (E.D. = 0,5 mm) is adequately positioned upstream the test model and a black opaque liquid dye is injected in the free flow, permitting the visualization of streaklines.

The second flow visualization method utilized in this work, named dye wash technique, employed liquid dye. Large amount of a dense black dye is injected close of the test model, enough to tint the entire flow field. Suddenly, the dye injection is stopped, the hypodermic needle is taken off the flow, in order to minimize flow perturbations. The clean water flow washes the entire flow field, except in the cylinder wake, since in this region the flow speed is significantly smaller than in other regions. This procedure allows, during some seconds, for the wake downstream the cylinder to be watched. According to Lindquist, (2000) and Campos-Silva *et al*. (1998), dye wash technique is strongly recommended for visualization of the recirculation zone near the leeward face of the solid obstacle.

4. EXPERIMENTAL APPARATUS DESCRIPTION

All experiments have been carried out in a low turbulence water tunnel, depicted in Figure 2. This apparatus, recently modified and described briefly in the work of Gonçalves & Vieira (1999), permits operation in continuous or in blow-down mode. In blow-down operation mode it is possible to obtain a relative low turbulence level (less than 0,10 % in the test section centerline). All tests described in this work have been carried through in blow-down operation. The vertical test section has $146 \times 146 \times 500$ mm of dimensions and permits to shelter cylinders of 6.35 mm of diameter provoking a blockage ratio of less than 5.2 %. An extensive description of water tunnel facility and flow visualization hardware, after recent modifications, is available in Lindquist (2000).

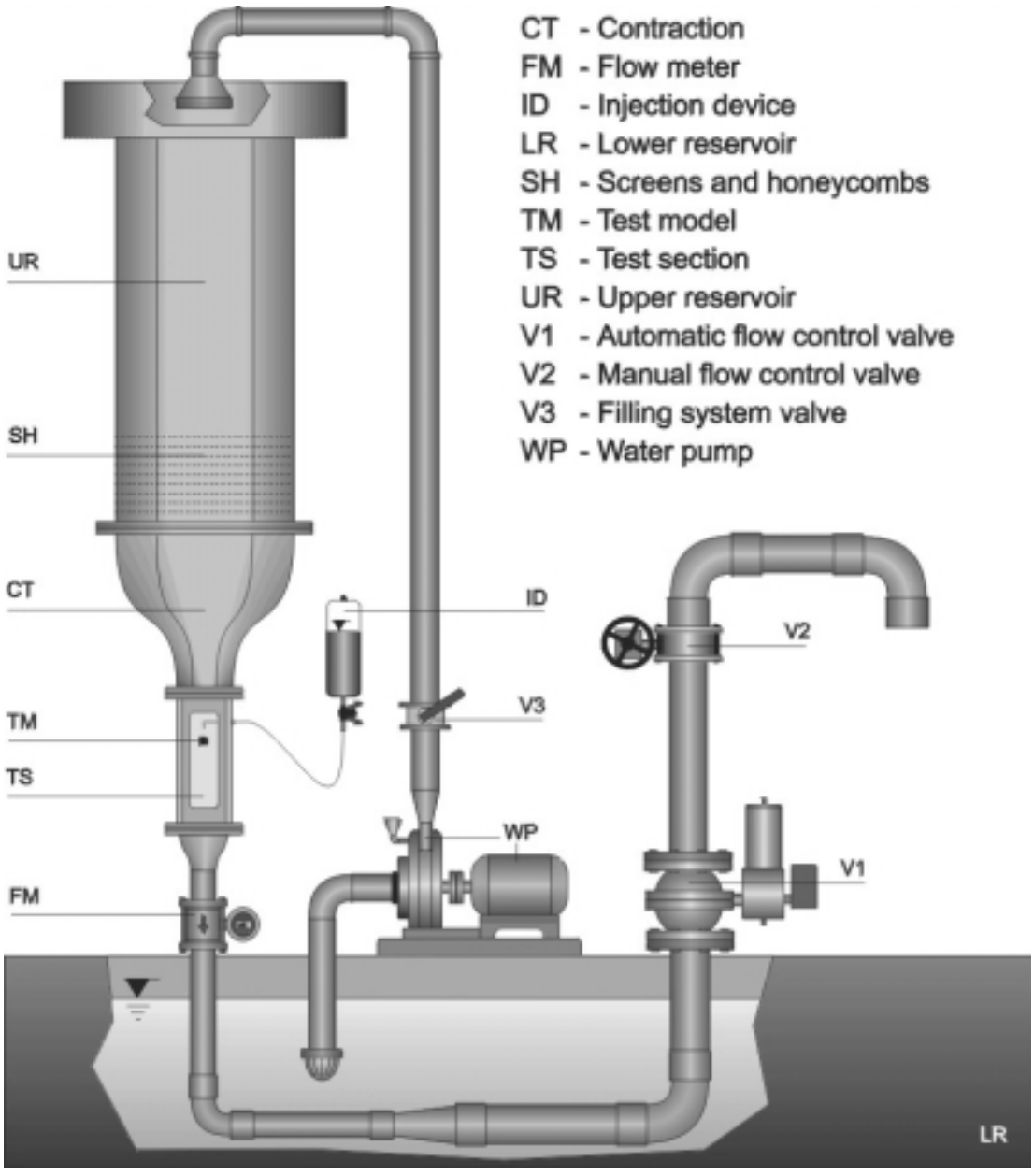

Figure 2 – Water tunnel facility.

The flow image has been illuminated by eight (150 W) *G.E. Photo Flood* tungsten lamps placed in line with the camera and shielded by white velvet-like translucent paper to provide a uniformly diffuse bright background against which the dye patterns were photographed. *Photo Flood* is a low-cost lamp, and supplies white light with high color temperature, adequate to capture images on a daylight type chemical photographic films. Unfortunately, *Photo Flood* is an incandescent type lamp that emits a high heat flux, requiring an air-cooling system, in order to prevent appreciable convection in the experiment.

The still images have been captured in a SLR (single lens reflex) *Nikon F4s* camera on 24×36 mm negative film, equipped with high luminosity *Nikor* macro 60 mm/f.1: 2.8 and a medical macro 120 mm objectives. The photos have been developed using *Kodak Ultra 400* (ISO 400) color negative films, with high contrast colors and high image definition, ideal for scanner reproductions.

Video tape images have been captured in a high resolution (over 800 horizontal lines) 3 CCD *KY-27 JVC* camera in order to determine the Strouhal "versus" Reynolds behavior of a single half-cane cylinder in two opposite angle of attack, i.e. the concave face turned upstream and downstream respectively. Equipped with a TC (time counter) board, this video camera permits to record a temporal identification of each frame. Observing, in a very controlled slow motion, the images recorded in video, it is possible to pinpoint easily the precise moment of the beginning of the vortex shedding process. Identified a complete vortex shedding period, time counter board permits to determine the time associated to the process and consequently the vortex frequency. An estimate of errors associated to vortex shedding frequency determination is about $\pm 5\%$. More details about the technique to determine the vortex shedding frequency using a VCR equipped with a time code reader board are presented in the work of Gonçalves & Vieira (1999).

The average velocity at the test section has been determined from the water flow rate measured by an electromagnetic flowmeter. This practice of determination of the average velocity in the test section measuring the downstream bulk flow rate is recommended by several authors, and currently used in many water tunnel facilities. The non-perturbed velocity, upstream the test model, has been obtained, in this work, using a *Yokogawa* electromagnetic flowmeter mounted downstream the test section. An assessment of the errors associated to free stream velocity has shown less than 5%, when compared with data obtained by hot film anemometer (*Dantec CTA Streamline*).

5. RESULTS

First of all, in order to understand the complex flow field in the inertial filter, we propose the study using visualization of the flow around a single semi-tube cylinder. The vortex wake images of a single semi-tube cylinder in two opposite arrangements are depicted in Figure 3, where the flow is vertical descendent. These flow images, which have been obtained using the dye wash technique, show sharply the wake downstream the test body. Obviously, as it can be clearly observed in Figure 3(a), the flow around of the concave face turned upstream produces a strongly recirculation-bubble. The liquid ink, trapped in the recirculation zone near the convex face leeward obstacle side, produces a very sharp black image and the vortices, along of von Kármán wake, are recorded smoothly in a weak grey tone. In this situation a particle trapped in the recirculation zone have a long sojourn time. In contrast, as observed in Figure 3(b), the wake image of the flow in the case when the test body with the convex face turned upstream shows a small recirculation zone and a very sharp vortex image.

(a) Concave face turned upstream
Re = 360

(b) Convex face turned upstream
Re = 225

Figure 3 – Flow visualization using dye wash technique of a single semi-tube cylinder in two opposite configurations.

(a) Concave face turned upstream
Re = 330

(b) Convex face turned upstream
Re = 88

Figure 4 – Flow visualization using direct liquid dye injection of a single semi-tube cylinder in two opposite configurations.

Figure 4 shows the flow images for the two arrangements proposed for single semi-tube cylinder using the injection of a filament line of opaque black dye directly in the free flow upstream the test model. In this flow visualization technique a streakline can be well visible and the process of vortex formation can be visualized. Additionally, it can be observed in the dynamic videotape images, that the convex face upstream positioned model produces high flow disturbances and a very unstable vortex wake, probably in function of the detachment that occurs in the sharp edge of the convex face.

The non-dimension vortex frequency for a single semi-tube cylinder has been obtained through the manual video image processing. The behavior of Strouhal number in function of Reynolds number is depicted in Figure 5 in two opposite attack angle.

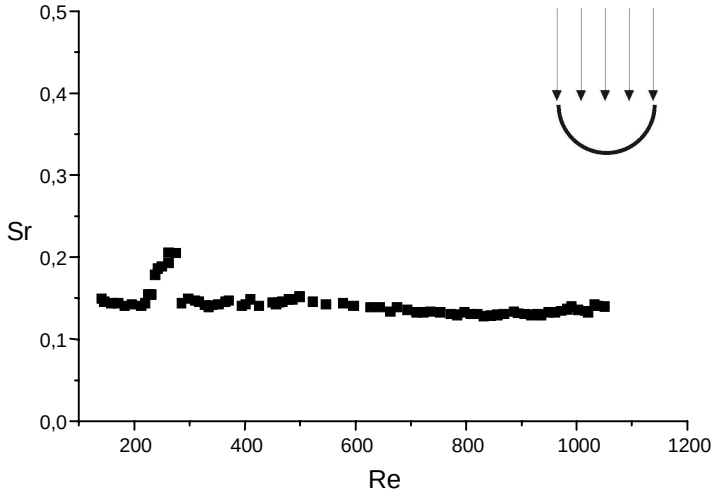

Figure 5 –Strouhal number in function of Reynolds number - concave face turned upstream.

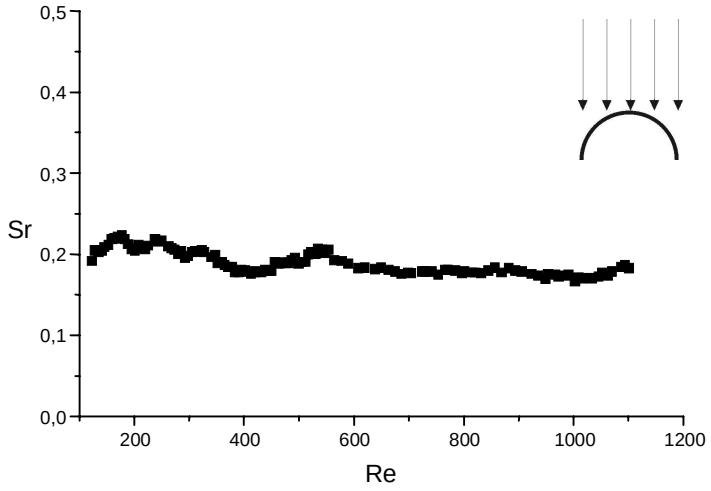

Figure 6 – Strouhal number in function of Reynolds number - convex face turned upstream.

The wake generated by the concave upstream face semi-tube cylinder is wider than the one generated in the opposite configuration. The relatively smaller vortex wake width allows for a higher iteration between the two shear layers, and this situation, apparently, yields a greater vortex shedding frequency.

In order to carry on the flow visualization studies, three semi-tube cylinders, in an arrangement similar searched in a trap filter, have been tested in the water tunnel. The flow images, for this situation is showed in Figure 7.

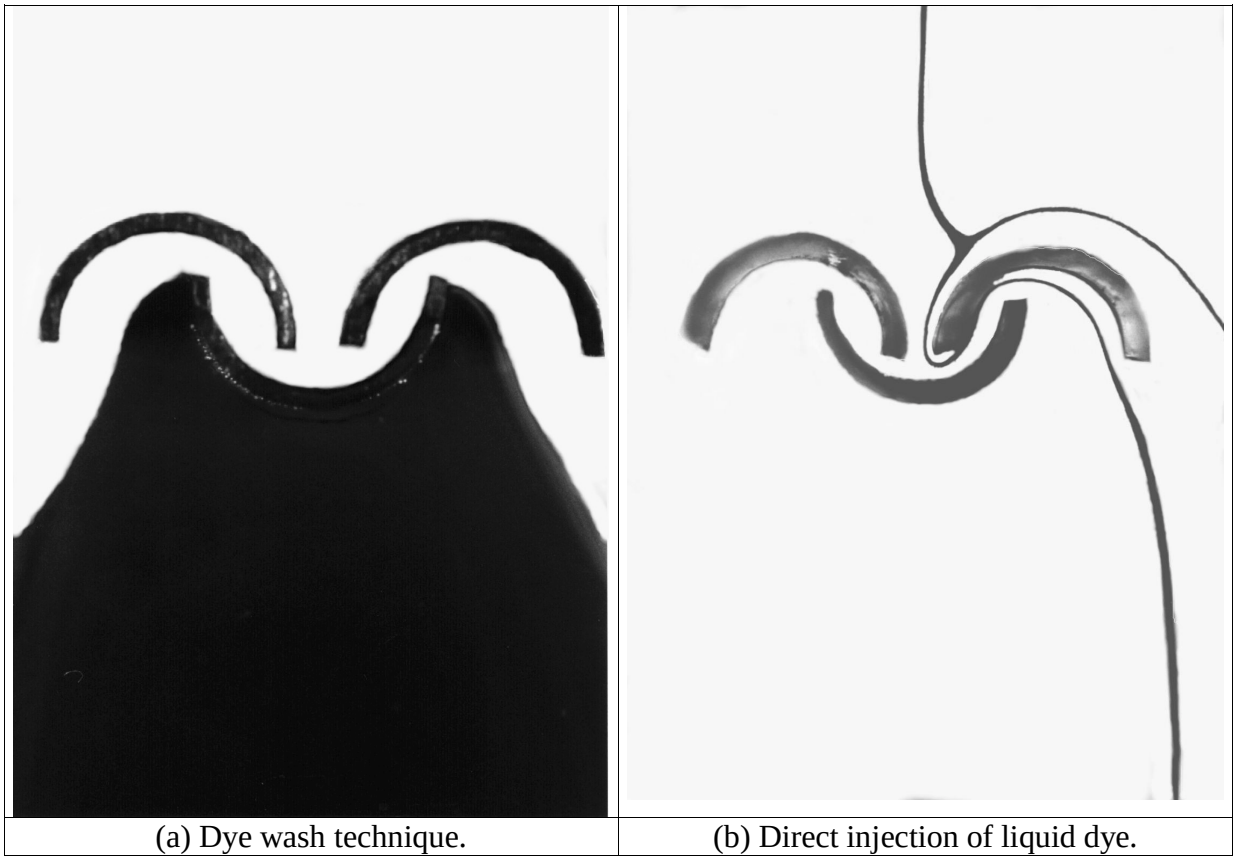

(a) Dye wash technique. (b) Direct injection of liquid dye.

Figure 7 – Hydrodynamic flow visualization in a trap filter model.

The flow images obtained in the model test showed in figure 7(a) using dye wash flow visualization technique reports a sharp wake provoked by a large recirculation zone. In other words, a micro oil drop arrested to this region has a high probability of shocking against the leeward walls of the trap filter. The same test run (Reynolds, based in diameter of the semi-tube cylinder, equal to 290), however utilizing direct injection of liquid dye, showed in Figure 7(b), reports a streakline in the centerline of the test model. The flow image shows a curved streakline with small curvature radius. The small radius produces high inertial forces over the oil drops, which are denser than the air, causing a high probability of oil drops shocks against the internal trap filter walls.

6. CONCLUSIONS

Experimental flow visualization plays a key role in our understanding of complex flow phenomena. That important experimental tool has been utilized in this working effort to obtain the first results of the study of flow in oil trap filters. A trap filter model has been positioned perpendicularly, in relation to non-perturbed flow, in the test section of a hydrodynamic tunnel and the flow field images have been captured using liquid dye flow visualization techniques. Still images permit obtains qualitative information about the flow

around a single semi-tube section in two different attack angle configurations and in an array of three semi-tubes. Videotape images processing, in the case of flow around a single semi-tube, has allowed for the Strouhal versus Reynolds curve determination in two attack angle arrangements.

In the present work, a number of questions remain unanswered, e.g. the discontinuity observed in the Strouhal curve showed in the Figure 5, in such a way that harder effort need to be made towards their solution.. Despite a thorough search by the authors, no references in scientific literature have been found to inertial filter behavior. On the other hand, Brazilian inertial filter manufacturers are in urgent need of corroborated results in order to satisfy global market requisites. There are some limitations in the present work, such as the relatively low Reynolds numbers of the tests and the reduced model dimensions, which play to difficult the visualization of the fine flow details. However, from a practical viewpoint, at the least this work might be used to encourage the manufacturers to engage on research programs in order to understand the operating principles of inertial filters and to obtain quantitative results.. Notwithstanding those shortcomings, the principal goal of this work has been totally achieved, i.e., to identify the action of droplet impact and diffusion as the principal oil trap mechanism. As for the future, the team is now planning a construction of a test facility bench operating with air as work fluid and employing hot wire anemometry to obtain quantitative results.

Acknowledgement

The experiments have been, in part, financed by FAPESP. Recognition is likewise due to Fundunesp and PROPP/Unesp.

REFERENCES

Campos Silva, J.B., Vieira, E.D.R. &. Moura, L.F.M., 1998, Control Volume-Finite Element and Flow Visualization Methods Applied for Unsteady Viscous Flow Past a Circular Cylinder. Proceedings of the V CEM NNE – V Congresso de Engenharia Mecânica Norte e Nordeste, vol.2, pp.80-87, Fortaleza, CE.

Erickson, G.E., 1980, Vortex flow visualization, AFWAL-TR-80-3143.

Freymuth, P., 1993, Flow visualization in fluid mechanics, Revue Science Instruments, vol 64, pp.1-18.

Goldstein, R.J. (ed.), 1976, Fluid Mechanics Measurements, Hemisphere Publishing Co., New York.

Gonçalves, H.C. & Vieira, E.D.R., 1999, Strouhal Number Determination for Several Regular Polygon Cylinders for Reynolds Number up to 600, Proceedings (in CD ROM) of the. COBEM 99 - XV Congresso Brasileiro de Engenharia Mecânica, *(paper code AACFFE*), 10 pp, Águas de Lindóia.

Lindquist, C., 2000, Estudo experimental do escoamento ao redor de cilindros de base quadrada e retangular, dissertação de mestrado, Unesp – Ilha Solteira.

Merzkirch, W., 1987, Flow Visualization, 2nd ed., , Academic Press, Orlando.

Schatzmann, M., 1999, Wind tunnel modeling of fog droplet deposition on cylindrical obstacles. Journal of Wind Engineering and Industrial Aerodynamics, vol.83, pp.371-380.

Yang, W.-J. (ed.), 1898, Handbook of Flow Visualization, Taylor & Francis, Ann Arbor.

Werlé, H., 1973, Hydrodynamic Flow Visualization, Annual Review of fluid Mechanics, vol.5, pp.361–382.